https://doi.org/10.15407/scine18.02.100

PROIDAK, Yu. S. (https://orcid.org/0000-0001-7380-055X),
GLADKYKH, V. A. (https://orcid.org/0000-0002-7279-8133),
and **RUBAN, A. V.** (https://orcid.org/0000-0001-6553-6568)
National Metallurgical Academy of Ukraine,
4, Gagarina Ave., Dnipro, 49600, Ukraine,
+380 56 745 3156, nmetau@nmetau.edu.ua

STUDYING THE PHASE EQUILIBRIA IN MnO-SiO$_2$ SYSTEM BY THE DIFFERENTIAL SCANNING CALORIMETRY (DSC) METHOD

Introduction. *The formation of rational composition of molten slag is critical for smelting of manganese ferroalloys. From seventy to ninety per cent of manganese ferroalloy slags are presented by manganese and silicon oxides. Information about phase equilibrium in $MnO—SiO_2$ system has an important value for the development of new and the improvement of operating processes of beneficiating and agglomerating manganese raw material, manufacturing manganese ferroalloys, and smelting high-manganese electrical steels.*

Problem Statement. *The analysis of scholarly research data on the diagram of the equilibrium state of $MnO—SiO_2$ system has shown a difference between the temperature of eutectic melting and that of peritectic melting and a fundamental difference in the nature of these two types of melting. The diagram does not show the polymorphic transformation of rhodonite.*

Purpose. *The purpose of this research is to study the behavior of manganese orthosilicate and metasilicate and the eutectic between them for specifying the structure of the $MnO—SiO_2$ system equilibrium state diagram.*

Materials and Methods. *The DSC method has been used to determine the temperature of phase transformations, melting and crystallization, of the samples that correspond to rhodonite ($MnSiO_3$), tephroite with rhodonite ($Mn_2SiO_4 + MnSiO_3$), and the eutectic located between them in terms of composition.*

Results. *The temperature of tephroite congruent melting, the solidus and the liquidus of rhodonite incongruent melting have been determined more accurately. For the first time, the temperature of rhodonite polymorphic transformation at the phase transition γ-$MnSiO_3 \leftrightarrow \beta$-$MnSiO_3$ accompanied with a volume fluctuation of up to 2% has been experimentally established. This has made it poss ible to plot the horizontal line of polymorphic transformation on the $MnO—SiO_2$ system diagram.*

Conclusions. *The obtained data on the equilibrium state of $MnO—SiO_2$ system have given a clear idea of the slag system structure, which allows us to optimize cooling during the manganese agglomerate production; to rationally select the slag melting conditions for the ferrosilicon manganese production; to improve slag thickening after the release of smelting products; to justify slag crystallization behavior for the production of slag-cast products.*

Keywords: $MnO—SiO_2$ system, DSC, phase equilibrium, γ-$MnSiO_3 \leftrightarrow \beta$-$MnSiO_3$, and polymorphic transformation.

Citation: Proidak, Yu. S., Gladkykh, V. A., and Ruban, A. V. (2022). Studying the Phase Equilibria in MnO—SiO$_2$ System by the Differential Scanning Calorimetry (DSC) Method. *Sci. innov.*, 18(2), 100—107. https://doi.org/10.15407/scine18.02.100

The formation of molten slag rational composition appears to be important for smelting manganese ferroalloys. In the electric steelmaking processes, usually, the slag ratio does not exceed 0.2 for smelting most ferroalloys (except for ferrosilicon). However, in the case of producing ferrosilicon manganese, the slag ratio is 1.2—1.4 and, in the case of producing medium-carbon ferromanganese and metallic manganese, it is 2.5—3.0. For the most part, in addition to manganese oxides (30—70%), the raw oxide manganese materials (ore, concentrate, agglomerate), contain waste rock that is mainly represented by silicon oxides (20—30%), calcium oxides (5—10%), and aluminum oxides (2—5%) [1]. Both the low-phosphorus slag (LFS) and manganese charge slag (MCS) obtained by the electrometallurgical dephosphorization, from fluxless smelting of high-carbon ferromanganese, contain 45—58% MnO and 25—35% SiO_2. In oxide melts of the above compositions, SiO_2 is the structurant [2], while MnO is the main inoculant. Therefore, the interaction between manganese oxides and silicon oxides is a key factor for the study of the physicochemical processes of manganese raw material beneficiation and agglomeration, as well as for the production of manganese alloys.

Recording the phase equilibria in the MnO—SiO_2 system is critical both for developing new and improving the existing processes of manganese raw material beneficiation, for manganese ferroalloy production, as well as for the high-manganese electrical steel smelting. In the MnO-SiO_2 system, there have been synthesized the two manganese compounds: Mn_2SiO_4 orthosilicate (70.92% MnO) and $MnSiO_3$ metasilicate (54.19% MnO) [3]. Mn_2SiO_4 orthosilicate corresponds to natural Mn olivine. The olivine group members are Mn_2SiO_4 tephroite ($Mn_{1,6}Fe_{0,4}SiO_4$), $Mn_{1,4}Fe_{0,6}SiO_4$ knebelite ($Mn_{0,6}Fe_{1,4}SiO_4$), and $MnCaSiO_4$ glaucochroite. $MnSiO_3$ metasilicate is isostructural neither with the olivine group, nor with $MgSiO_3$ and $CaSiO_3$.

The analysis of the diagrams of the equilibrium state of MnO—SiO_2 (Mn—S) system presented in

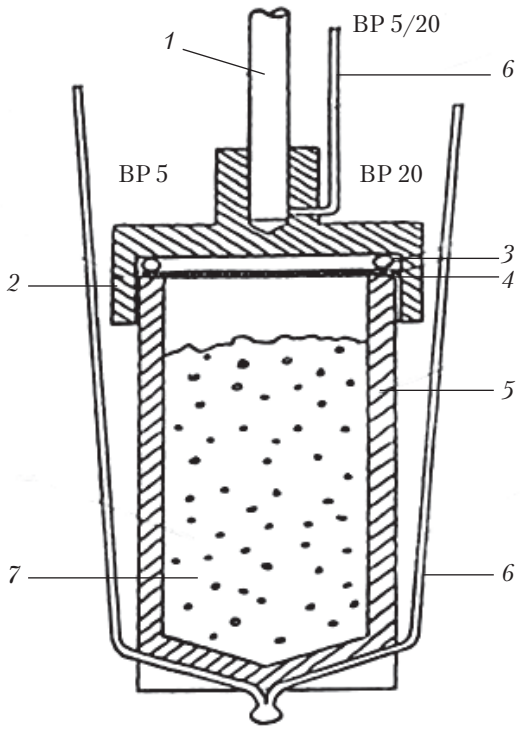

Fig. 1. DSC module: *1* — bearing tungsten rod; *2* — cover with a press-fit rod; *3* — ring of tungsten wire; *4* —molybdenum plate; *5* — crucible; *6* — thermocouples; *7* — sample

[3—11] has shown that in J. White's early publication [3], there is a diagram showing two peritectics melting incongruently: the first one (Mn_2SiO_4) on the side of MnO melts with decomposition to MnO + liquid, and the second one ($MnSiO_3$) on the side of SiO_2 melts with decomposition to SiO_2 + liquid. There has been shown one eutectic point between Mn_2SiO_4 and $MnSiO_3$.

The distinctive feature of the phase diagram by F.P. Glasser [5] is that Mn_2SiO_4 melts congruently, while $MnSiO_3$, as in the previous case, melts incongruently. In addition, this diagram shows two eutectics. *The first eutectic* (E1: 74.1% MnO, 25.9% SiO_2) located between MnO and Mn2SiO4 melts at a temperature of 1315 °C, and *the second one* (E2: 61.5% MnO, 38.5% SiO_2) located between Mn_2SiO_4 and $MnSiO_3$ melts at 1250 °C. Following the main features of F.P. Glasser's diagram, the authors [6] have calculated different values of temperature for eutectic and pe-

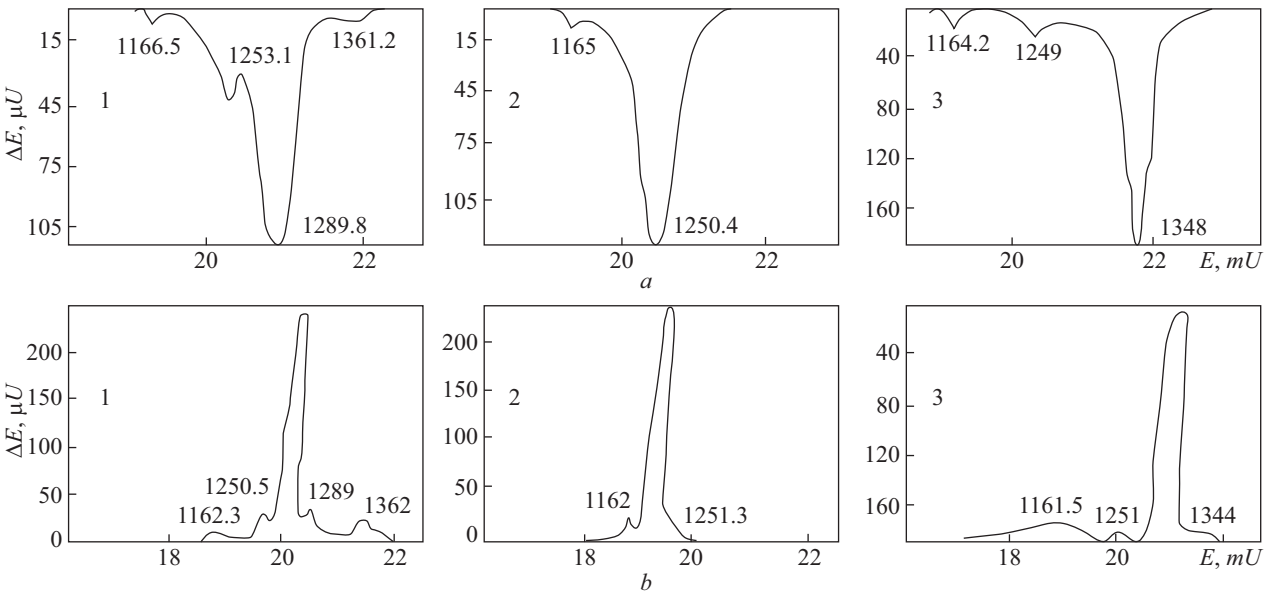

Fig. 2. DSC curves of the samples No. 1—3 (Table 1) of the MnO—SiO_2 system obtained by (*a*) heating and (*b*) cooling

ritectic melting. Moreover, the temperature and concentration boundaries of delamination into two liquids on the SiO_2 side have been specified.

There are records on the presence of the three modifications of rhodonite: α-, β-, γ-$MnSiO_3$, of which α-$MnSiO_3$ is metastable at normal pressure and within the whole range of temperature [12]. The parameters of the crystal structures of γ-$MnSiO_3$ and β-$MnSiO_3$ have been given. They virtually coincide with natural bustamite for β-$MnSiO_3$ [3]. However, none of the phase diagrams of MnO—SiO_2 system considered in the research works has featured this polymorphic transformation. At the same time, the phase diagrams of CaO—SiO_2 and Al_2O_3—SiO_2 systems show regions of modification transformations. In order to clarify the above features, we have studied the behavior of manganese orthosilicate and manganese metasilicate as well as the eutectic between them while heating and cooling them with the use of the differential scanning calorimetry method [13].

Table 1. **Chemical Composition of MnO—SiO_2 System Model Samples**

Element	Sample composition, %		
	$MnSiO_3$	Eutectic 2 (E2)	Mn_2SiO_4 + $MnSiO_3$
MnO	54.2	61.5	70.0
SiO_2	45.8	38.5	30.0

Differential scanning calorimetry (DSC) is used to determine the phase transition temperature, as well as the temperature of melting and crystallization for individual compounds and mixes thereof. In comparison with the differential thermal analysis (DTA) method, this one has much more reliable capabilities, accuracy, reproducibility of results, experimental data processing and interpretation, and phase identification [13].

The studies have been carried out on a DSC module to measure local differential temperature of the cell (Fig. 1). The device (that is differential in design) operates in the mode of temperature sheath scanning. The operating temperature ranges within 400—2080 °C, the possible heating rate varies from 5 to 100 °C/min. The calibration coefficient of the device is 20 μV/mW with a relative error of ± 0.5%, and it does not depend on the sample mass. The noise level is ± 0.5 μV. The sample weight is 6 g.

The samples are crushed, pressed into a pellet, and heated in a helium atmosphere at an automatically given rate of 50 mV/h in alundum crucibles that have been precalcined in a neutral atmosphere and reinforced with molybdenum foil. Having been melted, the samples are kept for 30 min. Then, the cooled samples are crushed to 0.2—0.4 mm, placed in a block connected to a differential thermocouple and heated. During the first heating, the indicators are not recorded. The measurements are carried out during cooling and reheating. If necessary, heating and cooling are repeated to check the consistency of the results without dismantling the block.

When two pure oxides are mixed, the melting point of the system decreases, therefore, the accurate record of the temperature allows us to determine theoretically the equilibrium compounds and the amount of impurities in the pure phase or, with a known composition, to predict the melting point.

Two methods have been used to make calculations of melting temperature of the mixes that are similar to the samples in terms of composition, which allows the correct interpretation of the results of the experiment in the MnO—SiO_2 binary system and its approximate control.

According to the first method, the calculation is done with the use of the Raoul-Van't Hoff equation [14]:

$$X_2 = A \cdot \Delta T, A = \frac{\Delta H_f}{RT_0^2}, \quad (1)$$

$$X_{2(\text{mole\%})} = 100 \cdot \frac{\Delta H_f}{RT_0^2} \cdot \Delta T, \quad (2)$$

where X_2 is the mole fraction of impurities in ideal liquid phase, A is the first cryoscopic constant

Table 2. **Test Parameters, Probable Temperature and Transitions in MnO (Mn)—SiO_2 (S) System**

Test No.	Composition, wt%. Test parameters	Temperature (°C), transitions			
1	54.2% MnO, 45.8% SiO_2.				
	Heating:	1166.5	1253.1	1289.8	1361.2
	740°C →1480°C	γ-MnS+E1 → β-MnS+ E1	β-MnS+ E1→ liquid + + β-MnS	β-MnS → liquid + + tridymite	liquid + tridymite → → liquid
	$V_{heating}$ = 15mV/h				
	Cooling:	1162.3	1253.1	1289.8	1361.2
	1480°C → 740	β-MnS + E1 → γ-MnS + E1	liquid + β-MnS → → β-MnS+ E1	liquid + tridymite → β-MnS	liquid → liquid + + tridymite
	$V_{cooling}$ = 15mV/h				
2	61.5% MnO, 38.5% SiO_2.				
	Heating:	1165.0	1250.4		
	700°C →1490°C	γ-MnS+Mn_2S → E1 (β-MnS+Mn_2S)	E1 (β -MnS+Mn_2S) → → liquid	—	—
	$V_{heating}$ = 15mV/h				
	Cooling:	1162.0	1251.3		
	1490°C → 700	E1 (β-MnS + Mn_2S) → → γ-MnS+Mn_2S	liquid → E1 (β-MnS+Mn_2S)		
	$V_{cooling}$ = 15mV/h				
3	70.3% MnO, 29.7% SiO_2.				
	Heating:	1164.2	1249.0		1348.0
	740°C →1570°C	γ-MnS+Mn_2S → E1+Mn_2S	E1+Mn_2S → Mn_2S+ + liquid	—	Mn_2S+ liquid → liquid
	$V_{heating}$ = 15mV/h				
	Cooling:	1161.5	1251.0		1344.0
	1570°C → 740	E1+Mn_2S → γ-MnS+Mn_2S	Mn_2S+ liquid → → E1 + Mn_2S		liquid → Mn_2S+ + liquid
	$V_{cooling}$ = 15mV/h				

Note: $V_{heating}$ — sample heating rate. $V_{cooling}$ — sample cooling rate.

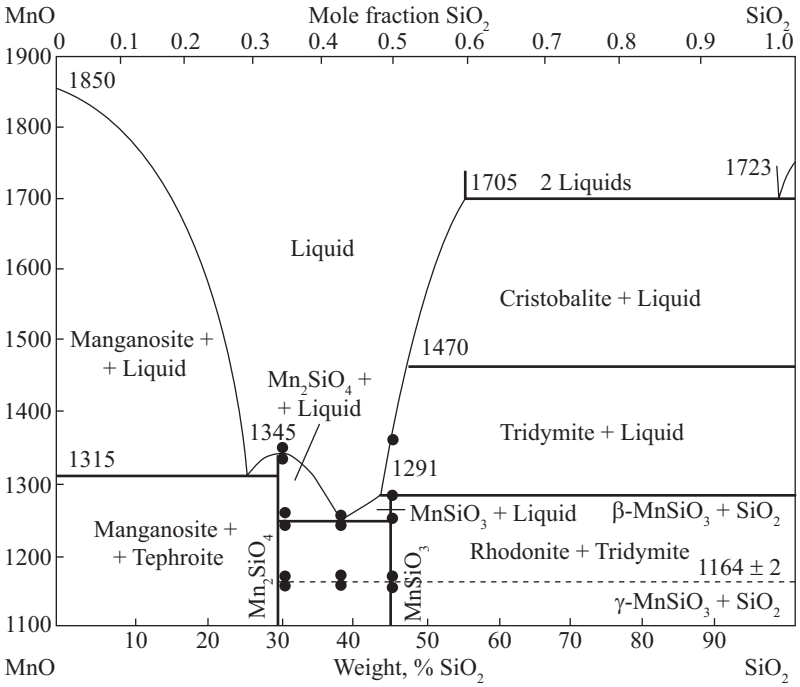

Fig. 3. Phase diagram of $MnO—SiO_2$ system: - - - - proposed line of the γ-$MnSiO_3 \leftrightarrow \beta$-$MnSiO_3$ polymorphic transformation; —— - data obtained by P.F. Glasser; ● - experimental data

(K^{-1}), ΔT is the melting point depression with respect to pure substance (K): ΔH_f is the fusion heat (enthalpy) of pure substance (J/mol), R is the universal gas constant (8.314 J/mol · K), T_0 is the melting point of pure substance (K).

In accordance with the second method, the Le Chatelier—Shreder equation is used [15]:

$$T = \frac{T_0}{1 - \frac{\ln X_i}{N_i}}, \qquad (3)$$

where X_i is the mole fraction of impurity component, N_i is the number of atoms in the formula of a compound.

The object of the study is represented by the samples that have the composition corresponding to that of $MnSiO_3$ rhodonite, Mn_2SiO_4 + + $MnSiO_3$ tephroite with rhodonite, and the eutectic located between them (Table 1). The transition temperature and the character thereof are given in Table 2 and in Fig. 2.

The inhomogeneous melting and crystallization (Fig. 2) indicate a gradual transition of the liquid structure into that of the crystalline state. Having a composition corresponding to tephroite, the melt consists of microclusters of the crystalline tephroite type, and its crystallization and melting are followed by ordering and disordering in the liquid. This phenomenon is clearly visible near the melting point on the DSC diagrams (Fig. 2, *b*). After ordering in the liquid during crystallization, there may be observed a rigidly vertical peak that corresponds to the crystallization of a chemical compound.

The smooth pattern of the eutectic crystallization (Fig. 2, *b*) is caused by the additional formation of rhodonite and tephroite from the liquid due to the redistribution of silica, since at eutectic melting, rhodonite is decomposed in the reaction:

$$Mn_2SiO_4 + Mn_5Si_5O_{15solid} \rightarrow 2\{2Mn^{2+} + [SiO_4]^{4-}\}liquid + \{3Mn^{2+} + [Si_4O_{11}]^{6-}\}liquid, \quad (3)$$

i.e. new clusters on the basis of $[SiO_4]^{4-}$ and $[Si4O_{11}]^{6-}$ silicon—oxygen motifs appear.

The transformations in the sample that corresponds to rhodonite in terms of composition are

stepwise. At the temperature of peritectic transformation (1290 °C), free silica release is followed by the simultaneous formation of a liquid from two clusters:

$$Mn_5Si_5O_{15solid} \rightarrow \{2Mn^{2+} + [SiO_4]^{4-}\}_{liquid} + \\ + \{3Mn^{2+} + [Si_3O_9]^{6-}\}liquid + SiO_{2solid}. \quad (4)$$

Further melting at the liquidus line at a temperature of 1362 °C is accompanied by the transformation of solid tridymite into a cluster:

$$(3Mn^{2+} + [Si_3O_9]^{6-})_{liquid} + SiO_{2\,solid} \rightarrow \\ \rightarrow (3Mn^{2+} + [Si_4O_{11}]^{6-})_{liquid}. \quad (5)$$

The proposed mechanism of polymorphic transformations in the solid and liquid states during melting and crystallization in $MnO-SiO_2$ system is logically interconnected with the concepts of the nature of the chemical bonding of silicon in manganese-silicate melts, which have been developed in [2, 16–19].

During polymorphic transformations, additional horizontal lines corresponding to the transformation points are plotted on the diagrams. These lines separate stability envelopes of individual modifications of the same compound. This phenomenon is observed if one of the components has two or more polymorphic modifications. As it has been mentioned, in $MnO-SiO_2$ system, $MnSiO_3$ rhodonite compound is represented by several modifications, two of which (γ-$MnSiO_3$ and β-$MnSiO_3$)

Table 3. **Comparative Characteristics of the $MnO–SiO_2$ System Phase Diagram Parameters Based on the Data Obtained in Various Studies**

Parameters, dimension	Value, characteristics, source			
	[2]	[4]	[5]	The study presented herein
Compound:				
— Mn_2SiO_4:				
Composition, %:				
MnO	70.92	70.92	70.92	70.30
SiO_2	29.08	29.08	29.08	29.70
Melting point, °C	1336	1345	1345	1316
Type of melting $MnSiO_3$:	incongruent	congruent	congruent	congruent
Composition, %:				
MnO	54.20	54.20	54.20	54.20
SiO_2	45.80	45.80	45.80	45.80
Solidus *t*, °C	1273	1291	1291	1290
Liquidus *t*, °C	none known	none known	1367	1361.6
Type of melting	incongruent	incongruent	incongruent	incongruent
Eutectic 1 ($MnO - Mn_2SiO_4$)	absent	present	present	present
Composition, %:	—	74.1	74.1	74.1
MnO	—	25.9	25.9	25.9
SiO_2	—	1315	1321	1315
Melting point, °C				
Eutectic 2 (Mn_2SiO_4 $MnSiO_3$)	present	present	present	present
Composition, %:	64.95	61.66	63.01	61.50
MnO	35.05	38.34	36.99	38.50
SiO_2	1230	1250	1251	1250.8
Melting point, °C				
Polymorphic transformation on the diagram, °C:				
Heating γ-$MnSiO_3 \rightarrow \beta$-$MnSiO_3$	absent	absent	absent	1164.2—1166.5
Cooling β-$MnSiO_3 \rightarrow \gamma$-$MnSiO_3$	absent	absent	absent	1161.5—1162.3
Mean *t* , °C	—	—	—	1164.0

are stable within a certain temperature range. However, this phenomenon is not plotted on any of the studied diagrams [5, 10—12]. We also have estimated the polymorphic transformation temperature that is consistent with that previously obtained [12]. The γ-$MnSiO_3$ ↔ β-$MnSiO_3$ polymorphic transformation occurs at a temperature of 1161—1166 °C that is below the eutectic point temperature. On the side of SiO_2, up to the vertical line of Mn_2SiO_4, there appears a temperature range of stability of γ- and β- modifications, which enables us to indicate this phenomenon on the phase diagram of the MnO—SiO_2 system (the dashed line) (Fig. 3). The comparative characteristics of the phase diagram parameters of the MnO—SiO_2 system (according to the data provided by various authors and those obtained in our studies) are given in Table 3.

Conclusions

1. The horizontal line at a temperature of 1164 °C, which reflects the γ-$MnSiO_3$↔ β-$MnSiO_3$ polymorphic transformation appears in the MnO—SiO_2 system phase diagram. It should be noted that this phenomenon is accompanied by a volume fluctuation of up to 2%.

2. The solidus temperature for incongruent melting of the 54.2% MnO and 45.8% SiO_2 composition that corresponds to rhodonite has been established; this temperature is equal to 1290 °C, and almost coincides with the diagram by P.F. Glasser (1291 °C).

3. The liquidus temperature of 1361.6 °C for the mix that corresponds to rhodonite in terms of composition has been determined more precisely.

4. The obtained values of the liquidus and solidus temperature of the studied compounds are precisely the same as those obtained in other studies. This fact confirms a high validity of the reflection of the γ-$MnSiO_3$ ↔ β-$MnSiO_3$ polymorphic transformation on the phase diagram of the MnO—SiO_2 system.

REFERENCES

1. Current Problems in Metallurgy. Vol. 19, Issue 1. (2016). *Scientific news*. Dnipropetrovsk: NMetAU, 290 p.
2. Gasik, M. I., Gladkikh, V. A. (1995). The Nature of the Chemical Bond of Silicon in Manganese Minerals and Manganese Silicates. *Report of the National Academy of Sciences of Ukraine*, 9, 60—63.
3. Gasik, M. I. (1992). *Manganese*. Moskow: Metallurgy. 608 p.
4. Slag Atlas. Reference work. Translated from German. Moskow: Metallurgy, 1985. 208 p.
5. Glasser, F. P. (1962). The Ternary System CaO-MnO-SiO_2. *O Amer. Ceram. Soc*., 5, 242—248.
6. Zaitsev, A. I., Mogutnov, B. M. (1997). Thermodynamics of Silicate Melts of the CaO—SiO_2 and MnO—SiO_2 System. *Modeling of Thermodynamic Properties and Calculation of Phase Equilibria/Inorganic materials*, 33(8), 975—984.
7. Sokolsky, V. E., Roik, A. S., Kazimirov, V. P., Pruttskov, D. V., Busko, V. M., Galinich, V. I., Goncharov, I. A. (2017). X-ray Diffraction Studies of Industrially Important Slag Melts at the Department of Physical Chemistry. *Bulletin of Donbass State Machine-Building Academy*, 2(41), 114—119.
8. Shpak, A. P., Sokolsky, V. E., Kazimirov, V. P., Smyk, S. Yu., Kunitskiy, Yu. A. (2003). *Structural Peculiarities of Oxide System Melts*. Kiev: Akademperiodika. 137 p.
9. Berezhnoy, A. S. (1970). *Multicomponent Systems of Oxides*. Kyiv: Naukova dumka. 456 p.
10. Herty, C. H., Conley, J. E., Royer, M. B. (1930). A Study of High-Manganese Slags in Relation to the Treatment of Low-Grade Manganiferous Ores. *Technical Papers #509*. Production of Explosives in U.S.: Department of commerce. 824 p.
11. Herty, C. H. (1931). A Practical Method of Solving the Emergency Manganese Problem. Rept. of Investigation 3107, Bureau of Mines. 714p.
12. Chemical Encyclopedia in 5 volumes. (1988). Vol. 1. Moskow: Sovetskaya entsyklopediya. 623 p.
13. Gaud, T. (1982). Fundamental of DSC: instruments and theory. *Comprehensive analytical chemistry*. Amsterdam, 12, B, 1155—1157.
14. Reznitsky, L. A. (1990). Thermochemistry of Anion-Deficient Perovskites and Compounds with a Brownmillerite Structure. *Journal of Physical Chemistry*, 64(9), 2228—2230.
15. Belov, N. V. (1961). *Crystal Chemistry of Large-Cation Silicates*. Moskow: Ed. Academy of Sciences of the U.S.S.R. Press, 405 p.
16. Gladkikh, V. A., Gasik, M. I. (2015). The study of silicon chemical bond in modeled silicate systems and manganese ores using x-ray photoelectron spectroscopy. *Energy efficiency and environmental friendliness are the future of the global Fer-*

roalloy industry: Proceedings of the Fourteenth International Ferroalloys Congress INFACON XIV. (May 31—June 4, 2015, Kiev, Ukraine). V. 2. Kyiv. 454—460.
17. Gasik, M. I., Gladkikh, V. A. (2015). The investigation of phosphorus chemical bond in the manganese-ore materials. *Energy efficiency and environmental friendliness are the future of the global Ferroalloy industry: Proceedings of the Fourteenth International Ferroalloys Congress INFACON XIV. (May 31—June 4, 2015, Kiev, Ukraine)*. V. 2. Kyiv. 470—478.
18. Sokol'skii, V. E., Kazimirov, V. P., Lisnyak, V. V., Roik, O. S., Goncharov, I. A., Galinich, V. I. (2015). *Welding Fluxes Structural and Physicochemical Aspects of Slag Melts*. Kyiv: PPC "The University of Kyiv". 239 c.
19. Gasik, M., Dashevskii, V., Bizhanov, A. (2020). *Ferroalloys. Theory and Practice. Topics in Mining. Metallurgy and Materials Engineering:* Springer Nature Switzerland. 531 p.

Received 05.05.2021
Revised 08.11.2021
Accepted 12.11.2021

Ю.С. Пройдак (https://orcid.org/0000-0001-7380-055X),
В.А. Гладких (https://orcid.org/0000-0002-7279-8133),
А.В. Рубан (https://orcid.org/0000-0001-6553-6568)
Національна металургійна академія України,
просп. Гагаріна, 4, Дніпро, 49600, Україна,
+380 56 745 3156, nmetau@nmetau.edu.ua

ДОСЛІДЖЕННЯ ФАЗОВИХ РІВНОВАГ В СИСТЕМІ $MnO—SiO_2$
МЕТОДОМ ДИФЕРЕНЦІАЛЬНО-СКАНУЮЧОЇ КАЛОРИМЕТРІЇ (ДСК)

Вступ. Під час виплавки марганцевих феросплавів важливе значення має формування раціонального складу шлакового розплаву. Шлаки марганцевих феросплавів на 70—90 % представлені оксидами марганцю та кремнію. Відомості про фазові рівноваги в системі $MnO–SiO_2$ є вагомим показником для розробки нових і вдосконаленні діючих процесів збагачення та огрудкування марганцевої сировини, отримання марганцевих феросплавів, а також виплавки електросталі з підвищеним вмістом марганцю.

Проблематика. Аналіз наведених в літературі даних стосовно діаграми рівноважного стану системи $MnO–SiO_2$ показав різницю температур евтектичного й перитектичного плавлення та принципову розбіжність у характері плавлення. На діаграмі відсутні дані щодо поліморфного перетворення родоніту.

Мета. Вивчення поведінки орто- і метасилікату марганцю, а також евтектики між ними для уточнення будови діаграми рівноважного стану системи $MnO–SiO_2$.

Матеріали та методи. Методом ДСК визначено температури фазових перетворень, плавлення й кристалізації зразків, що відповідають за складом родоніту ($MnSiO_3$), тефроіту з родонітом ($Mn_2SiO_4 + MnSiO_3$) та евтектиці, розташованої між ними.

Результати. Уточнено температури конгруентного плавлення тефроіта, солідус і ліквідус інконгруентного плавлення родоніту. Вперше експериментально визначено температуру поліморфного перетворення родоніту при фазовому переході $\gamma\text{-}MnSiO_3 \leftrightarrow \beta\text{-}MnSiO_3$, що супроводжується зміною об'єму до 2 %. Це дозволило нанести на діаграму стану системи $MnO–SiO_2$ горизонтальну лінію поліморфного перетворення.

Висновки. Отримані дані про рівноважний стан системи $MnO—SiO_2$ розширюють уявлення про будову шлакових систем, що дозволяє: оптимізувати процес охолодження під час виробництва марганцевого агломерату, раціонально підібрати шлаковий режим плавки при виробництві феросилікомарганцю, скорегувати процес загущення шлаку після випуску продуктів плавки, обґрунтувати режим кристалізації шлаку при виробництві шлаколитих виробів.

Ключові слова: система $MnO—SiO_2$, ДСК, фазова рівновага, поліморфне перетворення $\gamma\text{-}MnSiO_3 \leftrightarrow \beta\text{-}MnSiO_3$.